

Exploring the Interpretability of Forecasting Models for Energy Balancing Market

Oskar Våle, Shiliang Zhang, *Member, IEEE*, Sabita Maharjan, *Senior Member, IEEE*, Gro Klæboe

Abstract—The balancing market in the energy sector plays a critical role in physically and financially balancing the supply and demand. Modeling dynamics in the balancing market can provide valuable insights and prognosis to power grid stability and secure energy supply. While complex machine learning models can achieve high accuracy, their “black-box” nature severely limits the model interpretability. In this paper, we explore the trade-off between model accuracy and interpretability for the energy balancing market. Particularly, we take the example of forecasting manual frequency restoration reserve (mFRR) activation price in balancing market using real market data from different energy price zones. We explore the interpretability of mFRR forecasting using two models: (i) extreme gradient boosting machine (XGBoost) and (ii) explainable boosting machine (EBM). We also integrate the two models, and we benchmark all the models with a baseline naïve model. Our results show that EBM provides forecasting accuracy comparable to XGBoost while yielding a considerable level of interpretability. Our analysis also underscores the challenge of accurately predicting the mFRR price for the instances when the activation price deviates significantly from the spot price. Importantly, EBM’s interpretability features reveal insights into non-linear mFRR price drivers and regional market dynamics. Our study demonstrates that EBM is a viable and valuable interpretable alternative to complex black-box AI models in the forecast for the balancing market.

Index Terms—Energy balancing market, mFRR activation price forecasting, Explainable AI, model interpretability.

I. INTRODUCTION

A stable and reliable supply of electricity is crucial for the operation of any infrastructure in the modern society. The energy market plays a key role in maintaining grid stability by matching generation with consumption in real-time [1], [2]. Within this ecosystem, the balancing market is of critical importance for managing deviations, or power imbalances, that occur when planned operations differ from actual conditions [3], [4] due to uncertainties in the demand and supply, *e.g.*, renewable generation and vehicle charging and energy consumption [5], [6]. Vital balancing resources,

This work has been accepted by *Artificial Intelligence Science and Engineering*. DOI: 10.23919/AISE.2025.000020. This is a pre-print version.

Oskar Våle, Shiliang Zhang and Sabita Maharjan are with Department of Informatics, University of Oslo, Oslo, Norway (e-mail: oskar.vaale@gmail.com, {shiliang, sabita}@ifi.uio.no). Gro Klæboe is with Department of Electric Energy, Norwegian University of Science and Technology, Trondheim, Norway (e-mail: gro.kleboe@ntnu.no). This work was supported via the grant “Privacy preserving Transactive Energy Management (PriTEM)” funded by UiO:Energy Convergence Environments.

© 2025 IEEE. Personal use of this material is permitted. Permission from IEEE must be obtained for all other uses, in any current or future media, including reprinting/republishing this material for advertising or promotional purposes, creating new collective works, for resale or redistribution to servers or lists, or reuse of any copyrighted component of this work in other works.

e.g., Manual Frequency Restoration Reserve (mFRR), are activated to stabilize grid frequency when imbalance happens, and the cost to activate them is indicated by the activation prices [7]. Accurate forecasts of the balancing market are highly valuable to market participants for managing risk of high energy costs and for Transmission System Operators (TSOs) to ensure grid stability and reliability [8], [9]. Nevertheless, as the energy transition unfolds [10], modeling and predicting dynamics in the balancing market is increasingly challenging due to the integration of more variable renewables in the power grid, whose generation is intermittent and with uncertainties by its nature.

The evolving energy system has spurred the use of sophisticated forecasting methods, with machine learning (ML) offering powerful tools for identifying complex patterns in energy data [11]–[14]. Advanced ML models, such as the widely-used gradient boosting machine XGBoost [15], have demonstrated state-of-the-art performance in many energy forecasting applications. However, their high accuracy often comes at the cost of interpretability and renders them “black-box” models [16]. In critical domains like the energy balancing market, understanding why a model makes a certain prediction is necessary for deriving insights, ensuring transparency, and designing risk-mitigation measures [17]. This has fueled the growth of Explainable AI and the development of inherently interpretable “glass-box” models.

While literature exists on energy usage and price forecasting, studies specifically addressing the forecasting for the balancing market are rather sparse, more so when it comes to the accuracy-interpretability trade-off [18]. Some recent work has highlighted the challenges in predicting balancing market prices and volumes, suggesting limitations in accurate predictions using publicly available data [19]. In this paper, we address the gap by evaluating the trade-off between model prediction accuracy and interpretability for the balancing market. Particularly, we consider the forecasting of mFRR activation price, and we use the energy data of Norway’s five price zones which are with dominant renewables in its energy generation. We build models for the forecast, and we compare the performance of the state-of-the-art XGBoost model with an inherently interpretable alternative, and the explainable boosting machine (EBM) [20] which is designed to offer transparency through decomposable predictions without considerably compromising accuracy. To the best of our knowledge, we are the first to explore the accuracy-interpretability trade-off in forecasting balancing market dynamics.

We summarize the main contributions of this paper as: (i) evaluating the accuracy of the XGBoost model for mFRR

activation price forecasting across five price zones (ii) evaluating the performance of an inherently interpretable EBM model and that of a stacked EBM-XGBoost ensemble, where we explore the model accuracy-interpretability trade-off, and (iii) leveraging EBM’s interpretability to derive insights into non-linear price drivers and regional market dynamics.

The remainder of this paper is organized as follows. In Section II, we brief the background for mFRR activation price forecasting for the balancing market in Norway and the explainability of the forecast. In Section III, we describe about the models we considered in the forecast. In Section IV, we present the simulation setup and results, followed by analysis and discussions. Finally, Section V concludes the paper.

II. ACTIVATION PRICE PREDICTION AND EXPLAINABILITY

The energy balancing market aims to maintain real-time balance between electricity generation and consumption, ensuring operational security and system frequency stability [21]. In Norway, the balancing market is segmented into five distinct price zones from NO1 to NO5 [22], [23]. When deviations occur, the Norwegian national TSO Statnett activates balancing energy reserves to restore balance [24], [25]. In this paper, we look into the reserve of manual frequency restoration reserve (mFRR), and check the forecasting for it. The price paid for activating these reserves, in our example the mFRR activation prices, represents the marginal cost of this balancing action and is determined through the market [26]. Such activation prices compensate Balancing Service Providers (BSPs) and form the basis for settling the financial deviations of Balance Responsible Parties (BRPs) [27]. The mFRR activation price is inherently volatile and challenging to forecast accurately, as activations are driven by unforeseen deviations, real-time system needs, the magnitude of the imbalance, intermittence of production (especially by variable renewables), and transmission grid constraints [28].

As machine learning (ML) models become increasingly sophisticated and are deployed for such critical forecasting problems, the need for model interpretability becomes increasingly important [29], [30]. To this end, explainable AI (XAI) models are crucial not only for understanding the results, identifying biases and deriving insights, and but also for ensuring regulatory compliance - especially for critical domains like energy markets, and potentially also for discovering new domain-specific knowledge [31]. This study contrasts “black-box” models like XGBoost, which offer high performance but limited transparency, with “glass-box” models like the Explainable Boosting Machine (EBM), which provide inherent interpretability by design [32], [33]. For the structure, *e.g.*, of the EBM model, it allows for direct inspection of how individual features contribute to a prediction, offering transparency not readily available in more opaque models.

III. MODELS FOR MFRR ACTIVATION PRICE FORECASTING

To investigate the trade-off between predictive performance and model interpretability for mFRR activation price forecasting, we employ a set of carefully selected machine learning models. The choice of models was driven by the need

to benchmark against a simple approach, evaluate a high-performance “black-box” model, and thoroughly assess an inherently interpretable “glass-box” alternative. Below we describe these models along with their features, and the reason why we select them.

A. Naïve model

We adopt a naïve model where the forecast for the considered period is simply the last observed value. We use it as a baseline and we anticipate any sophisticated model should demonstrate significant improvement over this elementary approach.

B. XGBoost

XGBoost is a highly efficient and scalable implementation of the gradient boosting framework, which sequentially builds an ensemble of decision trees [32], [34]. Each new tree is trained to correct the errors of the previous ensemble. XGBoost is widely recognized for achieving high forecasting accuracy on various tabular datasets and serves as a robust benchmark for complex, yet often opaque models. XGBoost combines the predictions from multiple and often weak models, and creates a strong overall model. In XGBoost, models are sequentially trained where each new model corrects the errors made by the previous ones, and the training relies on gradients to improve the predictions. The sequential training of models results in the power of gradient boosting in XGBoost.

The objective function for XGBoost consists of (i) the loss function to be minimized and (ii) the regularization term. The objective function can be expressed as

$$\mathcal{L} = \sum_{i=1}^n \ell(y_i, \hat{y}_i) + \sum_{k=1}^K \Omega(f_k) \quad (1)$$

where n is the number of instances, y_i is the true label for instance i , \hat{y}_i is the predicted value for instance i , f_k represents the k -th tree in the ensemble, ℓ is the loss function measuring the difference between actual and predicted values, K is the total number of trees. $\Omega(f_k)$ is the regularization term for the complexity of each tree, usually defined as

$$\Omega(f_k) = \gamma T + \frac{1}{2} \lambda \|w_k\|^2 \quad (2)$$

where T is the number of leaves in tree k , γ is a parameter that controls tree complexity, λ is a regularization parameter, w_k are the leaf weights. During the construction of trees, XGBoost optimizes the objective function using a greedy algorithm. The resultant prediction is combined as

$$\hat{y}_i^{(t)} = \sum_{k=1}^t f_k(x_i) \quad (3)$$

where f_k is the prediction from the k -th tree, t is the current number of trees added to the model. To optimize the loss function, XGBoost uses first-order (gradient) and second-order (Hessian) derivatives of the loss function. Specifically, for a given prediction \hat{y}_i :

$$g_i = \frac{\partial \ell(y_i, \hat{y}_i)}{\partial \hat{y}_i} \quad (\text{gradient}) \quad (4)$$

$$h_i = \frac{\partial^2 \ell(y_i, \hat{y}_i)}{\partial \hat{y}_i^2} \quad (\text{Hessian}) \quad (5)$$

When finding the best split for a node, XGBoost computes the gain from splitting the data at a feature j

$$\text{Gain} = \frac{1}{2} \left(\frac{(\sum_{i \in \text{left}} g_i)^2}{\sum_{i \in \text{left}} h_i} + \frac{(\sum_{i \in \text{right}} g_i)^2}{\sum_{i \in \text{right}} h_i} - \frac{(\sum_{i=1}^n g_i)^2}{\sum_{i=1}^n h_i} \right) - \gamma \quad (6)$$

and the final predictions from the model can be expressed as

$$\hat{y}_i = \sum_{k=1}^K f_k(x_i) \quad (7)$$

While powerful, the resulting ensemble of many deep trees in XGBoost is often treated as a “black-box,” making it challenging to understand the precise reasoning behind its predictions.

C. Explainable boosting machine (EBM)

EBM is designed to be inherently interpretable while still leveraging the power of gradient boosting as is in XGBoost, making them ideal for exploring the performance-interpretability trade-off. EBM is a generalized additive model (GAM) that incorporates gradient boosting to learn each feature’s contribution [33]. The objective function in EBM follows a similar form to that of other boosting methods, but with a focus on producing additive models

$$\mathcal{L} = \sum_{i=1}^n \ell(y_i, \hat{y}_i) \quad (8)$$

where n is the number of instances, y_i is the true label for instance i , \hat{y}_i is the predicted value for instance i , ℓ represents the loss function. The predicted value \hat{y} from an EBM can be expressed as

$$\hat{y}_i = \sum_{j=1}^p f_j(x_{ij}) + \hat{y}_0 \quad (9)$$

where p is the number of features, f_j is the contribution from the j -th feature, x_{ij} is the value of the j -th feature for instance i , \hat{y}_0 is the global bias term or intercept. In EBM, each $f_j(x)$ can be represented as a smooth function, which allows for continuous relationships

$$f_j(x_{ij}) = f_j(\alpha_j) + f'_j(\beta_j)(x_{ij} - \alpha_j) \quad (10)$$

where α_j is a reference point for feature j , f_j is a parametric or non-parametric smooth function that maps the feature value to its contribution, f'_j denotes the derivative or slope of this function at the point α_j . EBMs maintain additivity across features, meaning that the impact of each feature on the prediction is independent of others. Therefore, the overall prediction can be easily interpreted as

$$\hat{y}_i = \hat{y}_0 + \sum_{j=1}^p f_j(x_{ij}) \quad (11)$$

The training process involves minimizing the loss function with respect to the model parameters using gradient boosting. For each boosting iteration t , the residual $r_i^{(t)}$ is calculated as

$$r_i^{(t)} = y_i - \hat{y}_i^{(t-1)} \quad (12)$$

and then fit the function f_j to the residuals, and the prediction can be updated as

$$\hat{y}_i^{(t)} = \hat{y}_i^{(t-1)} + \eta f_j(x_{ij}) \quad (13)$$

where η is the learning rate.

The primary advantage of EBM is its inherent interpretability. Global explanations are available through the ranked importance of each feature. Local explanations for individual predictions are derived by summing the contributions from each feature’s shape function for the given instance.

D. Stacked EBM+XGBoost model

We implement a stacked EBM+XGBoost model to assess whether combining the EBM’s predictions with an XGBoost model trained on its residuals can lead to further performance gains. In this ensemble model, we employ a two-level stacking architecture. The Level-0 base model is an EBM trained independently. The EBM’s residual $r_i^{(t)}$ in (12) on the training

TABLE I
DETAILED METRICS ON VALIDATION DATASET FOR MFRR ACTIVATION PRICE FORECASTS.

Upwards mFRR activation price forecasts													
Model Metric	MAE	Naïve			XGBoost			EBM			Stacked		
		MAE	R2	RMSE	MAE	R2	RMSE	MAE	R2	RMSE	MAE	R2	RMSE
no1	12.6252	-0.2389		45.4457	7.3639	0.5542	27.2610	7.2580	0.4453	34.9054	7.2976	0.4572	34.5303
no2	10.5150	0.5462		18.2591	4.6852	0.7921	12.4573	6.0851	0.7857	12.3654	4.7462	0.8081	11.7021
no3	8.4364	0.6105		17.0173	4.5368	0.8881	9.1221	8.2696	0.7323	13.5930	5.3416	0.8765	9.2351
no4	7.9726	0.6376		13.0649	5.5020	0.7159	11.5690	9.6987	0.5237	15.1106	6.3743	0.6862	12.2661
no5	9.2503	0.4964		20.8203	5.1325	0.7931	13.3444	6.4568	0.7969	12.2191	4.6942	0.8409	10.8138
Downwards mFRR activation price forecasts													
Model Metric	MAE	Naïve			XGBoost			EBM			Stacked		
		MAE	R2	RMSE	MAE	R2	RMSE	MAE	R2	RMSE	MAE	R2	RMSE
no1	10.0330	0.4807		22.1517	7.7712	0.5469	20.6908	9.5545	0.7208	14.1769	8.4438	0.7817	12.5360
no2	10.3121	0.4235		22.0653	7.6835	0.5785	18.8681	8.5140	0.7491	12.0150	7.2153	0.7808	11.2293
no3	8.0967	0.7082		12.9140	8.2782	0.7060	12.9621	9.3034	0.7440	12.2383	8.8894	0.7693	11.6170
no4	7.5834	0.6414		11.8028	8.1714	0.6799	11.1506	8.8006	0.7062	10.7175	8.7428	0.7081	10.6827
no5	8.4096	0.6562		13.7083	7.7181	0.6492	13.8469	10.4476	0.5913	14.9057	7.5929	0.6841	13.1047

TABLE II
DETAILED METRICS ON TEST DATASET FOR MFRR ACTIVATION PRICE FORECASTS.

Upwards mFRR activation price forecasts												
Model Metric	MAE	Naïve		XGBoost			EBM			Stacked		
		R2	RMSE	MAE	R2	RMSE	MAE	R2	RMSE	MAE	R2	RMSE
no1	14.973	0.3252	39.5797	8.9379	0.7051	26.1651	6.8112	0.7406	24.5423	6.7777	0.7404	24.5479
no2	16.0781	0.268	43.1884	4.8785	0.7703	24.1924	7.2108	0.7604	24.7102	4.7676	0.7703	24.195
no3	7.7871	0.2199	29.1914	4.9566	0.3656	26.3261	10.3383	0.2258	29.0811	4.8807	0.395	25.7086
no4	5.5549	0.0919	26.38	4.6359	0.1806	25.0596	6.85	0.1142	26.0545	4.7117	0.1607	25.3619
no5	12.0757	0.2787	35.6992	6.6637	0.6248	25.7489	7.7904	0.6444	25.0647	5.719	0.6455	25.0279
Downwards mFRR activation price forecasts												
Model Metric	MAE	Naïve		XGBoost			EBM			Stacked		
		R2	RMSE	MAE	R2	RMSE	MAE	R2	RMSE	MAE	R2	RMSE
no1	13.0629	0.4127	27.8561	6.9906	0.8297	14.9998	8.449	0.8338	14.8175	8.2953	0.8337	14.8245
no2	14.7361	0.2942	31.1818	8.8608	0.7722	17.715	10.4373	0.7372	19.0264	8.713	0.7018	20.2695
no3	6.0406	0.5103	13.2233	4.5606	0.7878	8.7041	6.2641	0.7279	9.8574	5.916	0.762	9.2182
no4	3.9839	0.4796	8.8056	4.1834	0.5976	7.7433	5.4147	0.548	8.2061	5.3485	0.5567	8.1269
no5	9.9953	0.444	21.7984	7.4878	0.8384	11.7531	7.7143	0.8349	11.878	5.2431	0.8621	10.8559

TABLE III
DETAILED METRICS ON TEST DATASET FOR MFRR ACTIVATION PRICE FORECASTS AFTER EXCLUDING PREDICTIONS FOR TIMES WHEN $spot = target$ FROM THE METRIC CALCULATIONS. N_{orig} AND N_{filter} INDICATE THE NUMBER OF ORIGINAL RECORDS AND FILTERED RECORDS, RESPECTIVELY.

Upwards mFRR activation price forecasts													
Area Metric	N_{orig}	N_{filter}	removed	Naïve	R2	RMSE	XGBoost	R2	RMSE	EBM	R2	RMSE	Stacked
				MAE			MAE			MAE			R2
no1	25504	7093	72.19%	18.3679	0.1230	56.0014	12.5790	0.4346	44.9635	11.3803	0.4362	44.9018	11.4199
no2	25504	5430	78.71%	21.1550	0.1047	60.6836	12.2021	0.3851	50.2912	12.8873	0.4045	49.4893	12.8415
no3	25504	5486	78.49%	12.6120	0.1027	54.9777	13.5348	0.1046	54.9177	13.8256	0.1462	53.6276	13.3269
no4	25504	6514	74.46%	11.1000	0.0929	47.3642	13.0213	0.0210	49.2051	14.1380	-0.0105	49.9916	14.0279
no5	25504	8026	68.53%	18.7463	0.1546	56.0016	12.0879	0.4676	44.4421	12.2542	0.5042	42.8878	12.0161
Downwards mFRR activation price forecasts													
Area Metric	N_{orig}	N_{filter}	removed	Naïve	R2	RMSE	XGBoost	R2	RMSE	EBM	R2	RMSE	Stacked
				MAE			MAE			MAE			R2
no1	25504	9809	61.54%	11.8341	0.2610	22.8703	13.4706	0.2539	22.9789	11.7285	0.3601	21.2811	11.7665
no2	25504	9133	64.19%	14.3753	-0.2346	28.4429	15.6579	-0.1192	27.0815	17.7922	-0.3128	29.3299	18.8288
no3	25504	9297	63.55%	5.9205	0.2990	12.0020	8.6507	0.1430	13.2710	8.7351	0.0556	13.9309	8.2264
no4	25504	11001	56.87%	4.7729	0.2509	10.1240	6.7444	0.1051	11.0655	6.1339	0.1926	10.5107	6.0740
no5	25504	8890	65.14%	9.8454	0.3452	17.7363	11.0979	0.4191	16.7051	10.9462	0.4083	16.8591	9.8746

set is then used as the target variable for the Level-1 meta-learner. The meta-learner was an XGBoost model, trained using the same input features as the EBM but tasked with predicting these EBM residuals. The final prediction from the stacked model for a given instance is the sum of the EBM's output and the XGBoost meta-learner's predicted residual.

IV. SIMULATIONS AND RESULTS

In this section, we describe the experimental setup, present the forecasting performance of the selected models in Section III, and elaborate on the key findings, particularly focusing on the accuracy-interpretability trade-off and insights derived from the EBM.

A. Dataset

The data for this study is sourced from the Value Insight API, covering the period from January 1, 2021, to March 15, 2025, from all the five Norwegian electricity price zones from NO1 to NO5. The dataset has a 15-minute temporal resolution. Key input features included the day-ahead spot price, forecasted consumption, forecasted hydropower and wind power production, forecasted residual load, forecasted heating and cooling needs, and cyclical temporal features (sine/cosine transformations of hour and month). The target variables to

be forecasted by our models are the 8-hour ahead mFRR activation prices for both upwards and downwards regulation. Upwards and downwards regulation mean to increase and to reduce power generation, respectively, in restoring demand-supply balance. We use an expanding window cross-validation approach for model training and validation. To simulate a realistic forecasting scenario, when generating predictions for the test set, input features (e.g., consumption, production) are based on forecasts available at the time of prediction, rather than actual yet unseen observed values.

B. Evaluation of model forecast accuracy

In this section, we evaluate the forecast accuracy of all the models forementioned in Section III. We use the metrics including Mean Absolute Error (MAE), Root Mean Squared Error (RMSE), and the Coefficient of Determination (R^2) in the evaluation. We select hyperparameters for XGBoost and EBM based on performance on a separate validation set by grid searching.

Table I and II show the performance of the considered models on the validation and test dataset, respectively. We observe from the tables that both XGBoost and EBM significantly outperform the Naïve baseline, demonstrating their capability to capture the complex dynamics of mFRR prices. Notably,

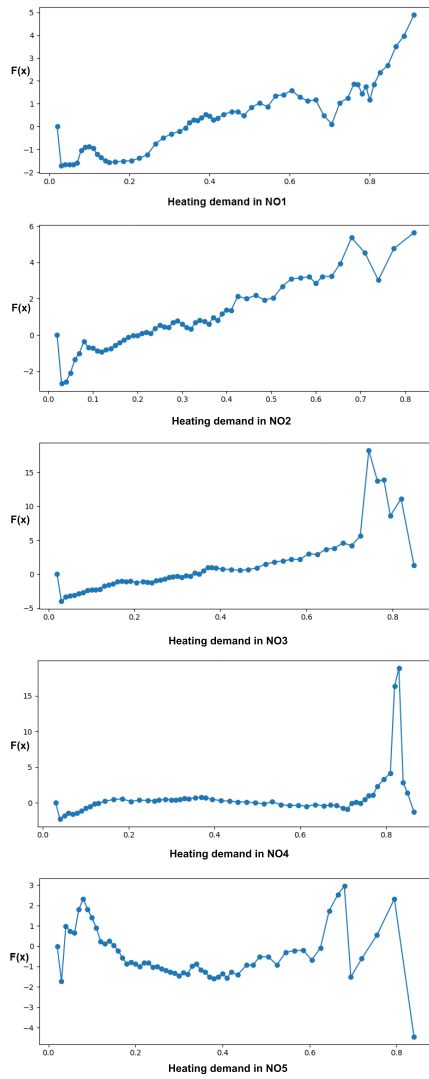


Fig. 1. Learned EBM feature shape $f(x)$ for heating demand in upwards mFRR across price zones.

EBM achieves an accuracy comparable to the more complex XGBoost model. The stacked EBM+XGBoost model offers marginal improvements over the best standalone models, and this improvement differs across the price zones. This suggests that with the current feature set, the EBM or XGBoost alone captured most of the predictable signal for zones like NO5 for the downwards mFRR and NO4 for upwards mFRR, while the stacked model extracts more features in other zones and scenarios.

A significant novel finding is the challenge in forecasting periods where activation prices deviate from the day-ahead spot price, which is a dominant feature in determine the mFRR price. When models are evaluated exclusively on these “deviation events” (representing a smaller fraction of total instances, yet of critical importance in risk analysis for the balancing market), performance for all models including EBM and XGBoost drops substantially, as shown in Table III. For instance, R^2 values often approached zero or became negative, indicating that the models struggle to explain the

variance in these specific yet critical price movements. This suggests that while those models can capture the general price level anchored by the spot price, predicting the timing and magnitude of significant departures remains a key difficulty with the current feature set.

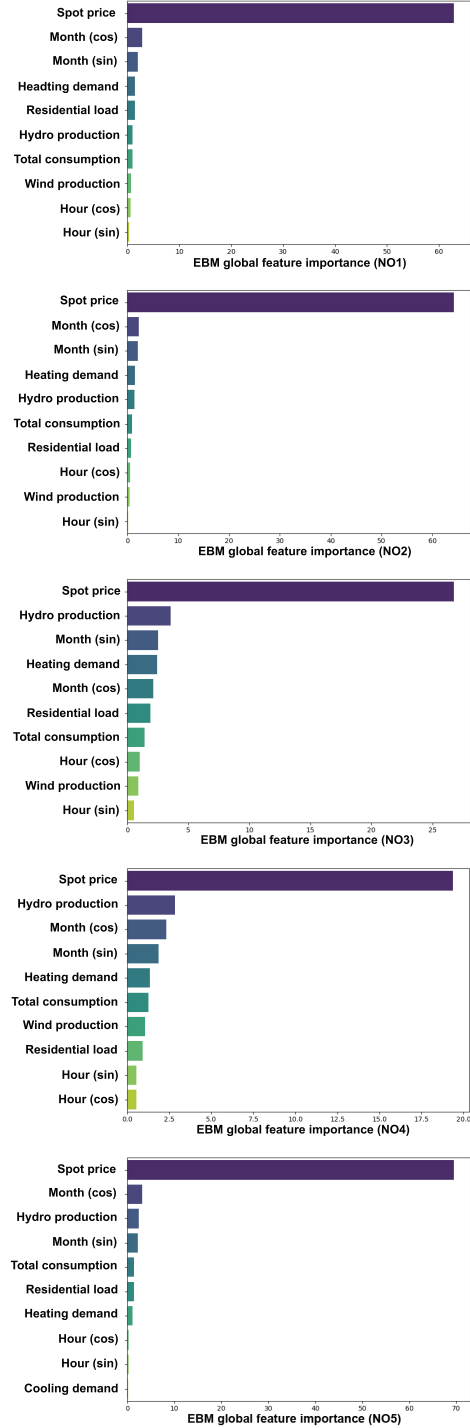


Fig. 2. Global feature importance plots for each price zone for the upward mFRR price by the EBM model. “Month (cos/sine)” represents cosine/sine component of the cyclical encoding for the month of the year, and “Hour (cos/sin)” indicates cosine/sine component of the cyclical encoding for the hour of the day.

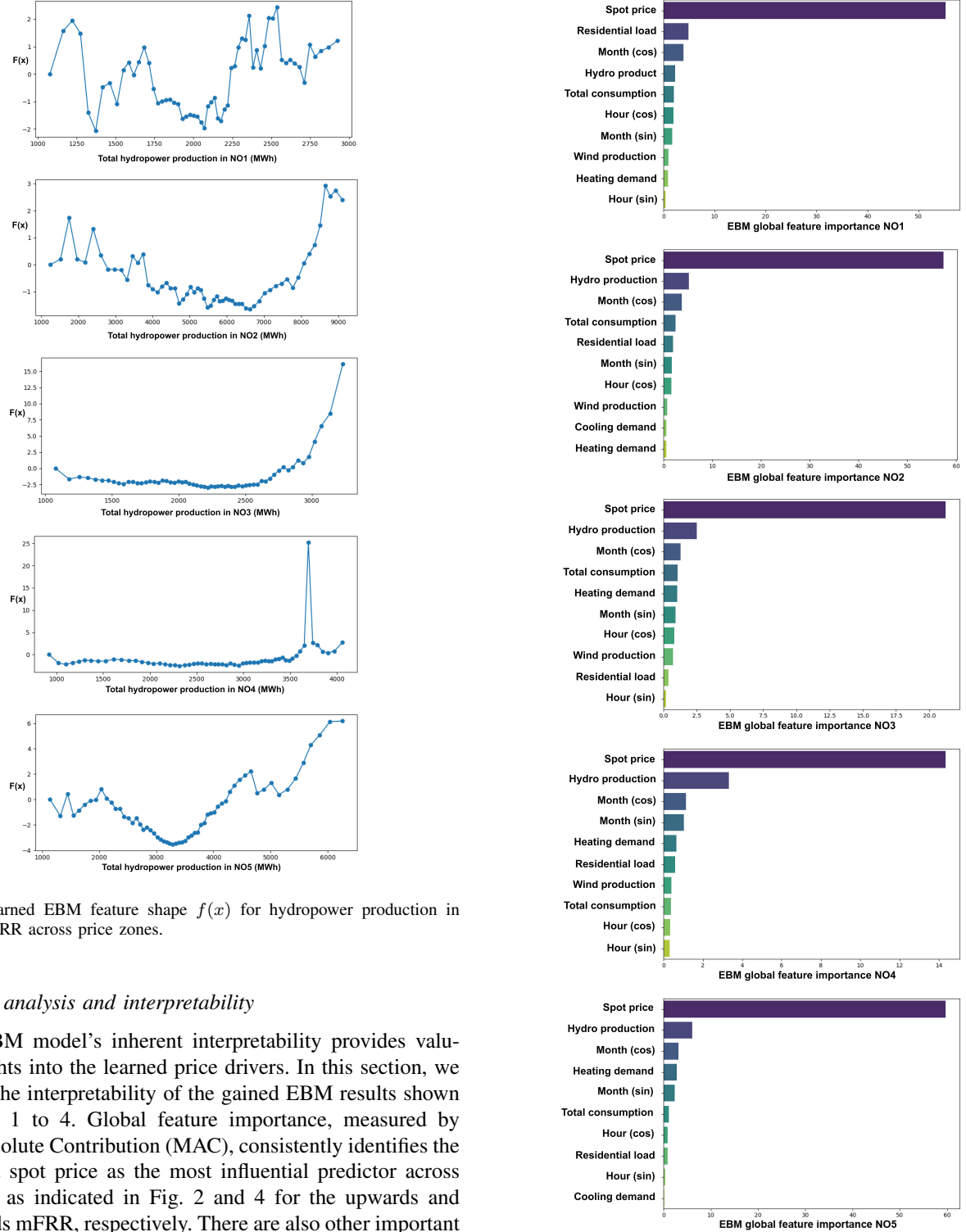


Fig. 3. Learned EBM feature shape $f(x)$ for hydropower production in upwards mFRR across price zones.

C. Result analysis and interpretability

The EBM model's inherent interpretability provides valuable insights into the learned price drivers. In this section, we illustrate the interpretability of the gained EBM results shown from Fig. 1 to 4. Global feature importance, measured by Mean Absolute Contribution (MAC), consistently identifies the day-ahead spot price as the most influential predictor across all zones, as indicated in Fig. 2 and 4 for the upwards and downwards mFRR, respectively. There are also other important features that come behind the spot price, *e.g.*, hydropower production (which consists of more than 80% of the total power generation in Norway), heating demand since it is necessary in the winter time, and temporal features that reflect seasonal energy consumption and production patterns. We also observe that the latter features take effect to different levels for different energy price zones across Norway. *E.g.*, hydropower production has a higher impact than seasonal factors in price zone NO3 and NO4, while not for NO1, NO2, and NO5. This corroborates the fact that NO3 and NO4 in Norway

have sufficient production of hydropower, while are with less population than NO1, NO2, and NO5. This leads to the higher contribution of hydropower in NO3 and NO4 in local energy supply and its higher impact in the balancing market. While in NO1, NO2, and NO5, which are all in the southern part

of Norway, they have a larger population that leads to higher heating demand in winter time, thus a higher impact of heating demand in the balancing market.

We show the relationship between upwards mFRR activation price and heating demand in Fig. 1, and that between upwards mFRR activation price and hydropower production in Fig. 3, respectively. Such a relationship is indicated by the shape function learned by the EBM model. Fig. 1 displays near-linear positive relationship between mFRR and heating demand in price zone NO1 and NO2, reflecting that the large population and comparatively less energy generation in NO1 and NO2 induces high heating demand and uncertainties in the heating demand to be compensated by the balancing market.

Fig. 3 shows that the impact of hydropower production does not have a significant impact on upwards mFRR activation price in NO3 and NO4, especially when the hydropower production is in a lower or mild level. This reflects that the sufficient hydropower generation in NO3 and NO4 does not add much uncertainties in the power grid that requests compensation by the balancing market. While in NO1, NO2, and NO5, the comparatively large population leads to more uncertainties in energy demand that needs to be compensated, and non-regular patterns can be observed for the relationship between mFRR activation price and hydropower production.

V. CONCLUSIONS

This paper addressed the trade-off between accuracy and interpretability for mFRR activation price forecast in the Norwegian energy market. Our results demonstrated that an inherently interpretable “glass-box” model, the explainable boosting machine (EBM), yields an accuracy of prediction comparable to the state-of-the-art “black-box” XGBoost model. The key implication of this work is that EBM can provide comparable accuracy to XGBoost while also yielding significant interpretability in balancing market predictions, providing direct insights into linear and non-linear price drivers and regional market dynamics that would otherwise be obscured. While this study underscores the potential of explainable AI, it also highlights that accurately predicting price deviations from the spot price remains challenging, largely due to the limitations of the current feature set. Future work should therefore focus on incorporating richer feature sets like real-time grid constraints, while also further exploring alternative model architectures.

REFERENCES

- [1] Laszlo Szabo, Magda Moner-Girona, Arnulf Jäger-Waldau, Ioannis Koulias, Andras Mezosi, Fernando Fahl, and Sandor Szabo. Impacts of large-scale deployment of vertical bifacial photovoltaics on european electricity market dynamics. *Nature Communications*, 15(1):6681, 2024.
- [2] Xiaobin Cheng, Pengfei Liu, and Lei Zhu. The impact of electricity market reform on renewable energy production. *Energy Policy*, 194:114306, 2024.
- [3] Enrique Rosales-Asensio, David Borge Diez, and Paula Sarmento. Electricity balancing challenges for markets with high variable renewable generation. *Renewable and Sustainable Energy Reviews*, 189:113918, 2024.
- [4] Selahattin Murat Sirin and Berna N. Yilmaz. The impact of variable renewable energy technologies on electricity markets: An analysis of the Turkish balancing market. *Energy Policy*, 151:112093, 2021.
- [5] Shiliang Zhang and Elad M Schiller. Privacy-preservation and the automotives. In *2020 AutoSPADA workshop, Gothenburg, Sweden*, 2020.
- [6] Shiliang Zhang. An energy consumption model for electrical vehicle networks via extended federated-learning. In *2021 IEEE Intelligent Vehicles Symposium (IV)*, pages 354–361. IEEE, 2021.
- [7] Dávid Markovics, Martin János Mayer, and Tamás Bessenyei. Short-term imbalance forecasting with machine learning for proactive mFRR controlling. In *2024 9th International Youth Conference on Energy (IYCE)*, pages 1–6, 2024.
- [8] B. Uzum, Y. Yoldas, S. Bahceci, and A. Onen. Comprehensive review of transmission system operators–distribution system operators collaboration for flexible grid operations. *Electric Power Systems Research*, 227:10976, 2024.
- [9] Shiliang Zhang, Sabita Maharjan, Lee Andrew Bygrave, and Shui Yu. Data sharing, privacy and security considerations in the energy sector: A review from technical landscape to regulatory specifications. *arXiv preprint arXiv:2503.03539*, 2025.
- [10] Daniel Gerbi Duguma, Juliana Zhang, Meysam Aboutalebi, Shiliang Zhang, Catherine Banet, Cato Bjørkli, Chinmayi Baramashetru, Frank Eliassen, Hui Zhang, Jonathan Muringani, et al. Privacy-preserving transactive energy systems: Key topics and open research challenges. *arXiv preprint arXiv:2312.11564*, 2023.
- [11] Shiliang Zhang, Dyako Fatih, Fahmi Abdulqadir, Tobias Schwarz, and Xuehui Ma. Extended vehicle energy dataset (eved): an enhanced large-scale dataset for deep learning on vehicle trip energy consumption. *arXiv preprint arXiv:2203.08630*, 2022.
- [12] T. A. Rajaperumal and C. Christopher Columbus. Transforming the electrical grid: the role of AI in advancing smart, sustainable, and secure energy systems. *Energy Inform.*, 8(1):51, 2025.
- [13] Jinbao Wang, Jun Liu, Shiliang Zhang, and Xuehui Ma. Ultra-short-term solar power forecasting by deep learning and data reconstruction. *arXiv preprint arXiv:2509.17095*, 2025.
- [14] Shiliang Zhang, Dyako Fatih, Fahmi Abdulqadir, Tobias Schwarz, and Xuehui Ma. Extended vehicle energy dataset (eved): An enhanced large-scale dataset for vehicle energy consumption analysis. In *2025 IEEE 101st Vehicular Technology Conference (VTC2025-Spring)*, pages 01–07. IEEE, 2025.
- [15] Jin-Xian Liu and Jenq-Shiou Leu. LARSI-TPE-XGB: Short-Term Load Forecasting by Load-Adaptive Relative Strength Index and Fusion of Tree-Structured Parzen Estimator and XGBoost. *IEEE Transactions on Power Delivery*, 40(3):1318–1330, 2025.
- [16] Suchit Gupte and John Paparrizos. Understanding the black box: A deep empirical dive into shapley value approximations for tabular data. *Proc. ACM Manag. Data*, 3(3), June 2025.
- [17] Bin Liu, Dan Wang, Jiawei Huang, and Chengxiong Mao. Optimal FNN-based energy management system with high real-time performance and good interpretability for battery in grid-connected microgrid. *IEEE Transactions on Industrial Electronics*, pages 1–12, 2025.
- [18] Shiliang Zhang, Sabita Maharjan, Raul Shahi, and Xuehui Ma. The impact of integration of renewable energy on imbalance settlement: Resilience analysis. In *2024 IEEE International Conference on Communications, Control, and Computing Technologies for Smart Grids (SmartGridComm)*, pages 98–104, 2024.
- [19] Stian Backe, Signe Riemer-Sørensen, David A. Bordvik, Shweta Tiwari, and Christian Andre Andresen. Predictions of prices and volumes in the Nordic balancing markets for electricity. In *2023 19th International Conference on the European Energy Market (EEM)*, pages 1–6, Lappeenranta, Finland, June 2023. IEEE.
- [20] Changhong Jin, John Upton, and Brian Mac Namee. Exploring explanation deficits in subclinical mastitis detection with explainable boosting machines. *Discover Agriculture*, 3(1):1–20, 2025.
- [21] M. Arun, Susmita Samal, Debabrata Barik, Sreejesh S.R. Chandran, Kapura Tudu, and Seepana Praveenkumar. Integration of energy storage systems and grid modernization for reliable urban power management toward future energy sustainability. *Journal of Energy Storage*, 114:115830, 2025.
- [22] Shiliang Zhang, Sabita Maharjan, Kai Strunz, and Jan Christian Bryne. Norwegian electricity in geographic dataset (noregeo). *arXiv preprint arXiv:2510.09698*, 2025.
- [23] Shiliang Zhang and Sabita Maharjan. Norwegian electricity in geographic dataset (noregeo)[dataset]. *Zenodo*, September 2025.
- [24] Tobias Verheugen Hvidsten, Maximilian Roithner, Fred Espen Benth, and Marianne Zeyringer. Driving towards net-zero: The impact of electric vehicle flexibility participation on a future Norwegian electricity system. *Environmental Research: Infrastructure and Sustainability*, 2025.
- [25] Nordic Balancing Model. BSP - Implementation Guide mFRR energy activation market. Technical report, Nordic Balancing Model, April 2024.

- [26] Milad Mousavi, Manuel Alvarez, Jin Zhong, and Sarah Rönnberg. Effects of flexibility contracts on manual frequency restoration reserve market considering transmission system flexibility issues. *International Journal of Electrical Power & Energy Systems*, 166:110576, 2025.
- [27] Konstantinos Plakas, Nikos Andriopoulos, Dimitrios Papadaskalopoulos, Alexios Birbas, Efthymios Housos, and Ioannis Moraitis. Prediction of imbalance prices through gradient boosting algorithms: An application to the Greek balancing market. *IEEE Access*, 13:103968–103981, 2025.
- [28] Nordic Balancing Model. Memo Algorithm description Nordic mFRR EAM bid selection v2. Technical report, Nordic Balancing Model Programme, November 2024.
- [29] Christoph Molnar. *Interpretable Machine Learning*. 2nd edition, 2022.
- [30] Shiliang Zhang and Sabita Maharjan. Cenergy3: An API for city energy 3D modeling. *arXiv preprint arXiv:2512.06459*, 2025.
- [31] Scott M. Lundberg and Su-In Lee. A Unified Approach to Interpreting Model Predictions. In *Advances in Neural Information Processing Systems 30 (NIPS 2017)*, pages 4765–4774. Curran Associates, Inc., 2017.
- [32] Tianqi Chen and Carlos Guestrin. XGBoost: A Scalable Tree Boosting System. In *Proceedings of the 22nd ACM SIGKDD International Conference on Knowledge Discovery and Data Mining*, pages 785–794. ACM, 2016.
- [33] Harsha Nori, Samuel Jenkins, Paul Koch, and Rich Caruana. InterpretML: A unified framework for machine learning interpretability. In *Workshops at the Thirty-Third AAAI Conference on Artificial Intelligence*, 2019.
- [34] Trevor Hastie, Robert Tibshirani, and Jerome Friedman. *The Elements of Statistical Learning: Data Mining, Inference, and Prediction*. Springer Series in Statistics. Springer, second edition, 2017.